Available online at www.sciencedirect.com
ScienceDirect
Bioorganic & Medicinal Chemistry 16 (2008) 2726–2733
Bioorganic & Medicinal Chemistry

A comparative density-functional study of the reaction mechanism of the O_2-dependent coproporphyrinogen III oxidase

Pedro J. Silva[a] and Maria João Ramos[b,*]

[a]*REQUIMTE, Fac. de Ciências da Saúde, Univ. Fernando Pessoa, Rua Carlos da Maia, 296, 4200-150 Porto, Portugal*
[b]*REQUIMTE, Faculdade de Ciências do Porto, Rua do Campo Alegre, 687, 4169-007 Porto, Portugal*

Received 28 November 2007; revised 2 January 2008; accepted 8 January 2008
Available online 11 January 2008

Abstract—During heme biosynthesis, coproporphyrinogen III oxidase catalyzes the conversion of two propionate substituents from the highly reactive substrate coproporphyrinogen III into vinyl substituents, yielding protoporphyrinogen IX. Although the crystal structure of this important enzyme has recently been reported, the reaction mechanism of this intriguing enzyme remains the subject of intense speculation, as impairment of this enzyme has been shown to be the molecular cause behind hereditary coproporphyria. We have performed DFT calculations on model systems in order to analyze several reaction mechanisms proposed for this enzyme. The results afford a full description of the different proposals and allow the rejection of a direct electron abstraction from the *protonated* substrate by dioxygen. We found that O_2 addition to the (preferentially deprotonated) pyrrole substrate (yielding a hydroperoxide, which then abstracts a proton from the reactive propionate substituent) is compatible with the observed experimental reaction rate, and that the reaction may then proceed through HO_2^- elimination, followed by decarboxylation.

1. Introduction

Deficient activities of the enzymes in the heme biosynthetic pathway often lead to tissue accumulation and excessive excretion of porphyrins or their precursors. These products are not only useless, but also toxic, and the ensuing diseases (collectively termed porphyrias) can be neurological or photosensitive, depending on the principal site of expression of the specific enzymatic defect.[1] Hereditary coproporphyria is an autosomal dominant porphyria due to decreased activity of coproporphyrinogen III oxidase, the sixth enzyme in the heme biosynthesis pathway. Symptoms include abdominal pain, neuropsychiatric symptoms, and/or cutaneous photosensitivity.[2] If diagnosed early, hereditary coproporphyria can be treated with a high carbohydrate diet and i.v. administration of heme in the form of heme arginate.[3]

Coproporphyrinogen III oxidase (E.C. 1.3.3.3.) catalyzes the oxidative decarboxylation of propionic acid side chains of rings A and B of coproporphyrinogen[4–7] (Fig. 1) without using metals,[8] reducing agents, thiols, prosthetic groups, organic cofactors, or modified amino acids.[9] The enzyme functions as a dimer in solution, and both the human[10] and yeast[11] enzymes have been crystallized and solved at good resolutions (2.0 Å for the yeast enzyme and 1.58 Å for the human variant). However, the mechanism by which the propionate side chains are converted to vinyl groups is presently poorly understood. Two mechanisms have been proposed: in the mechanism proposed by Arigoni,[10] the reaction proceeds through a one-electron oxidation of the substrate by oxygen, followed by H atom abstraction from the propionate side chain by the superoxide anion thus formed. Decarboxylation would then follow, with the electron-deficient pyrrole acting as an electron sink (Fig. 2A). In contrast, Lash[12] has proposed that the deprotonated form of the pyrrole ring would be able to attack dioxygen, and the formed 2*H*-pyrrole peroxide anion might abstract a proton from the propionate substituent, thereby allowing decarboxylation (Fig. 2B).

A large body of research on the applicability of density-functional (DFT) methods to enzyme-catalyzed oxidation reactions is available, usually on systems involving transition metals,[13,14] and with explicit treatment of all potential energy surfaces of the relevant multiplicities.[15,16] However, the reaction catalyzed by copropor-

Keywords: Coproporphyrinogen oxidase; Mechanism; Decarboxylation; Minimum-energy crossing point; Density-functional theory.
* Corresponding author. E-mail: mjramos@fc.up.pt

0968-0896/$ - see front matter © 2008 Elsevier Ltd. All rights reserved.
doi:10.1016/j.bmc.2008.01.008

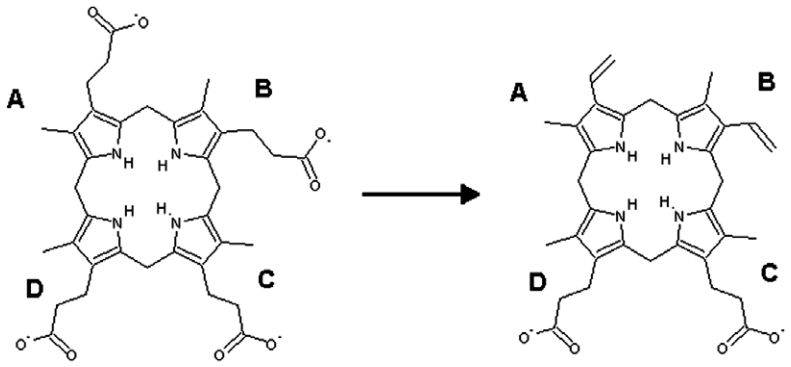

Figure 1. The reaction catalyzed by coproporphyrinogen oxidase.

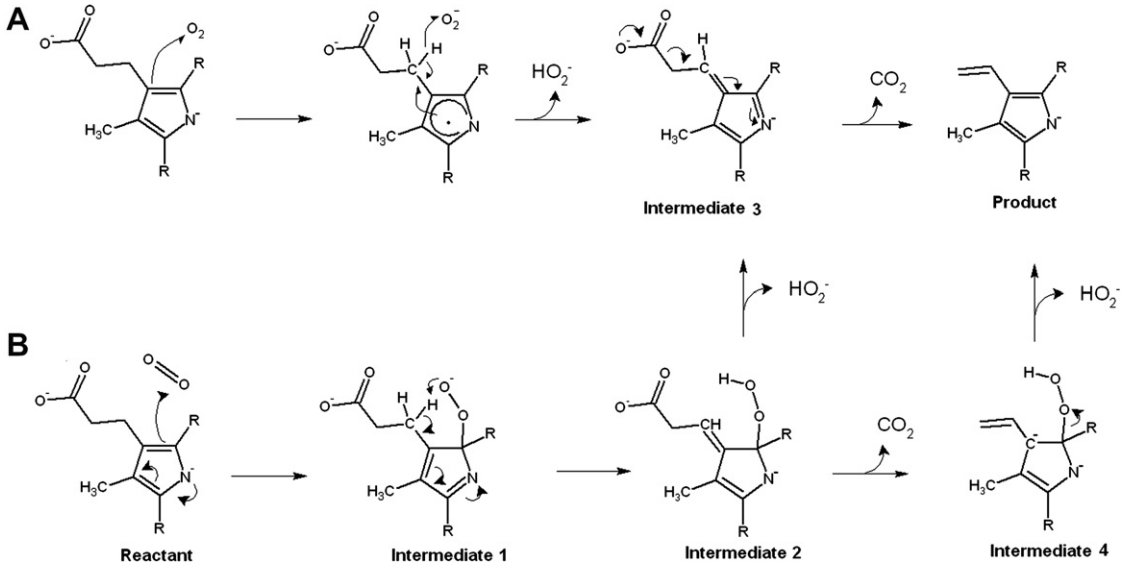

Figure 2. Proposed reaction mechanisms for coproporphyrinogen oxidase. (A) Arigoni model.[10] (B) Lash model.[12]

phyrinogen III oxidase has never been subjected to quantum chemical treatments. In order to test the proposed mechanisms, we carried out DFT calculations of both reaction mechanisms on N-deprotonated and N-protonated systems. Our calculations seem to favor the Lash mechanism, identify the rate-limiting steps of the different mechanistical proposals, and show that HO_2^- release must occur before decarboxylation.

2. Results

Despite recent progress in the identification of amino acids involved in catalysis and/or substrate binding to coproporphyrinogen III oxidase,[17,18] the absence of a three-dimensional structure of substrate-bound enzyme precludes the study of the (proposed) initial substrate deprotonation step due to the lack of knowledge regarding the precise amino acid acting as base and of surrounding amino acids which might modulate its pK_a (or that of the substrate). We have therefore performed quantum chemical computations on both the Arigoni and the Lash models, using either N-protonated or N-deprotonated pyrrole substrates. The results show that for the protonated substrate the reaction sequence arising from the Arigoni model is prohibitively expensive, in contrast to the Lash mechanism. For the unprotonated substrate the results seem to favor the Lash model (see below).

2.1. Arigoni model

The identification of transition states for pure electron-transfer reactions (i.e., electron transfers unaccompanied by significant atom movement) is very challenging due to the difficulty in constraining the orbital occupancies along reaction coordinates without major nuclear displacements. Therefore, we have calculated the activation energy of the one-electron transfer between the coproporphyrinogen III substrate and O_2 by applying Marcus theory for electron transfer, as suggested by Blomberg and Siegbahn.[19] The calculation of the activation energy of an electron-transfer reaction according to Marcus theory requires the knowledge of the reaction energy and of the reorganization energy of the system. Enthalpies are used here instead of free energies because for the reorganization energy it is not possible to determine the entropy effects. The reason for this is that in the calculation of the reorganization energy the structures do not correspond to equilibria, since for each part of

the system, the reorganization energy was obtained using the reactant's structure for the product state, and the product structure for the reactant state. The intersection of the Marcus parabolas built using these data yielded very small activation energies and confirmed the feasibility of the proposed electron transfer, provided that the pyrrole substrate is deprotonated (Table 1). The following step, however, is markedly slower, as the transition step for H· abstraction by O_2^- lies too high in energy (Fig. 3).

The intermediate arising from H· removal by O_2^- (intermediate 3) is also involved in the alternative Lash mechanism (see below). This intermediate decarboxylates readily upon extension of the C–COO^- bond to 2.29 Å, yielding the final product. The transition state for this step lies only 10.6 kcal mol^{-1} above intermediate 3 and is not rate-limiting. The overall sequence has an activation energy between 28.4 kcal mol^{-1} ($\varepsilon = 4$) and 19.4 kcal mol^{-1} ($\varepsilon = 78.3$) (Fig. 4). It is possible that the pyrrolyl radical formed from deprotonated substrate may react in many unexpected ways and therefore leads to the formation of novel species. However, no experimental support for the generation of different reaction products could be found in the literature, which leads us to believe that those reactions are either too slow (and therefore not competitive with protoporphyrinogen IX formation) or that the pyrrolyl radical formation is prevented by some feature of the enzyme active site. We therefore elected not to pursue the study of those possible reactions due to their presumed irrelevance for the enzyme reaction mechanism.

2.2. Lash model

2.2.1. 1st step: O_2 addition to the pyrrole anion. In Lash's model, coproporphyrinogen III oxidation begins with the addition of a (triplet) O_2 molecule to the (singlet) substrate. Starting from the deprotonated substrate, the minimum-energy crossing point between these two potential energy surfaces (Fig. 5) lies only 8.2 kcal mol^{-1} above the reactant state. At the crossing point, the difference of gradients along the C–O bond is 28.5 kcal mol^{-1}/Å, and there is a very strong (77.45 cm^{-1}) spin–orbit coupling between both states, yielding a very high transition probability between both surfaces and at most a 2.5 kcal mol^{-1} increase in the barrier due to the avoided crossing. This computed barrier is consistent with the experimental value (16 kcal mol^{-1}), calculated from the values reported by

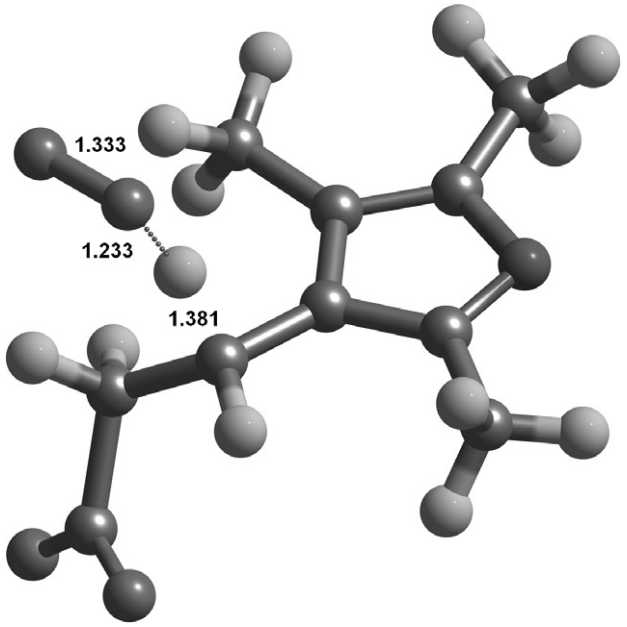

Figure 3. Structure of the transition step for H abstraction by O_2^- (TS 2 in the Arigoni model). Relevant distances are shown (in Å).

Medlock and Dailey[8] using the well-known Eyring equation:

$k_{cat} = \frac{k_B T}{h} e^{-\frac{\Delta G^{\ddagger}}{RT}}$, where k_{cat} is the measured rate constant, k_B is the Boltzmann constant, h is the Planck constant, and $\Delta G^{\ddagger}$ is the activation free energy.

In the case of a protonated pyrrole substrate, the minimum-energy crossing point lies 16.9 kcal mol^{-1} above the reactant state. Its geometry is markedly different from the corresponding structure in the deprotonated state: the O_2 molecule now lies much closer to the substrate C3. At this crossing point the spin–orbit is almost equal to the deprotonated case (77.35 cm^{-1} vs 77.45 cm^{-1}), and so is the difference of gradients along the C–O bond (31 kcal mol^{-1}/Å). As in the deprotonated state, this avoided crossing increases the barrier by at most 2.6 kcal mol^{-1}. The total electronic barrier in this case is 16.9 + 2.6 = 19.5 kcal mol^{-1} and therefore is slightly larger than the experimental value. The singlet–triplet gap at the computed minimum-energy crossing point is 0 kcal mol^{-1} at the B3LYP/6-31G(d) level, $\varepsilon = 4$. Its value increases slightly to 1.0 kcal mol^{-1} (protonated substrate) and 1.4 kcal mol^{-1} (deprotonated substrate) at the higher B3LYP/6-311+G(2d,p) level ($\varepsilon = 4$).

Table 1. Relative electronic energies (kcal mol^{-1}) of the reactants and products of the first step in the Arigoni model, calculated at the B3LYP/6-311+G(2d,p)//B3LYP/6-31G(d) level, for the N-deprotonated pyrrole substrate

	Gas phase		$\varepsilon = 4$		$\varepsilon = 20$		$\varepsilon = 78.3$	
	Energy	Reorganization energy	Energy	Reorganization energy	Energy	Reorganization energy	Energy	Reorganization energy
Pyrrole substrate + O_2	0.0	18.7	0.0	18.8	0.0	18.9	0.0	18.9
Pyrrole radical + O_2^-	−36.7	16.3	−10.5	9.5	−3.8	14.2	−2.5	14.1
Activation energy	8.1		<0.1		2.3		2.8	

Activation energies are calculated relative to the reactant state (pyrrole substrate + O_2). For the N-protonated pyrrole substrate, the reactions are strongly endergonic (42.0 kcal mol^{-1} at $\varepsilon = 4$; 36.0 kcal mol^{-1} at $\varepsilon = 20$, 34.6 kcal mol^{-1} at $\varepsilon = 78.3$).

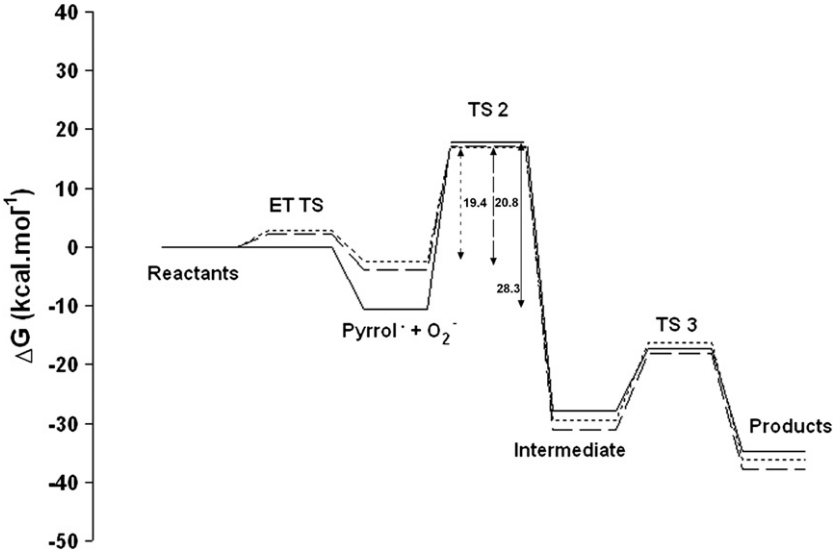

Figure 4. Overall reaction energy profile of coproporphyrinogen oxidase (Arigoni model with deprotonated substrate) at the B3LYP/6-311 + G(2d,p)//B3LYP/6-31G(d) (—) $\varepsilon = 4$; (---) $\varepsilon = 20$; (· · · · · ·) $\varepsilon = 78.3$.

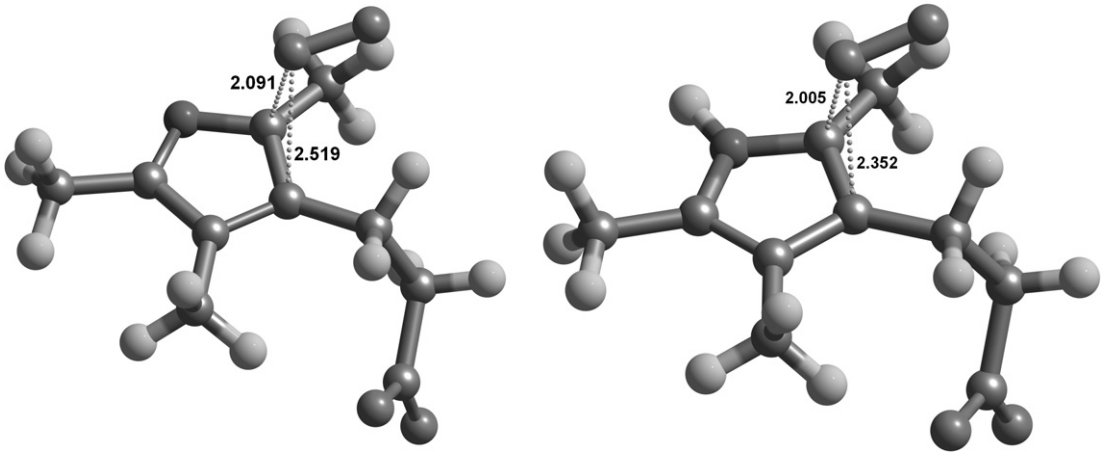

Figure 5. Structure of the minimum-energy crossing points between the singlet and triplet potential energy surfaces for Lash model (deprotonated substrate, left; protonated substrate, right). Relevant distances are shown (in Å).

2.2.2. Oxidative decarboxylation of pyrrole-peroxide (N-deprotonated pyrrole). The pyrrole peroxide anion (intermediate 1) formed in the previous step may easily remove a proton from the propionate substituent. This step (Fig. 6a–c) has an activation energy of 12.3 kcal mol^{-1} and is slightly endergonic (4.4 kcal mol^{-1}). Intermediate 2, formed in this reaction, then has two possibilities to decay into the final reaction product: it may decarboxylate first, and then shed a hydroperoxide anion, or it may eliminate the hydroperoxide before losing CO_2. CO_2 elimination as the first step is strongly discouraged: the negative charge present in the pyrrole system prevents the new negative charge arising from COO^- conversion into CO_2 from being stabilized by delocalization, which makes this step endergonic by 32.7 kcal mol^{-1} (Fig. 6d).

The search for a transition state for the hydroperoxide removal from intermediate 2 revealed a first-order saddle point (Fig. 6e) whose imaginary frequency corresponds to a movement of hydroperoxide roughly parallel to the pyrrole plane, accompanied by a methyl substituent rotation. Since this saddle point does not lie in the correct reaction coordinate, we added an explicit water (H_2O) molecule to our system in order to facilitate the search for the real transition state by stabilizing the developing negative charge on the peroxide (as active site amino acids are expected to do in the enzyme). The new search proved successful: a transition state lying only 0.9 kcal mol^{-1} above its reactant state and with the correct imaginary frequency was found at a pyrrole-hydroperoxide distance of 1.872 Å. HO_2^- elimination is strongly exergonic by 31.1 kcal mol^{-1}. Decarboxylation of the reaction product (intermediate 3) is exergonic by 6.9 kcal mol^{-1} and occurs readily with an activation ΔG of 10.6 kcal mol^{-1}.

2.2.3. Oxidative decarboxylation of pyrrole-peroxide (N-protonated pyrrole). In the case of O_2 adition to a N-protonated pyrrole substrate, gas-phase calculations predict

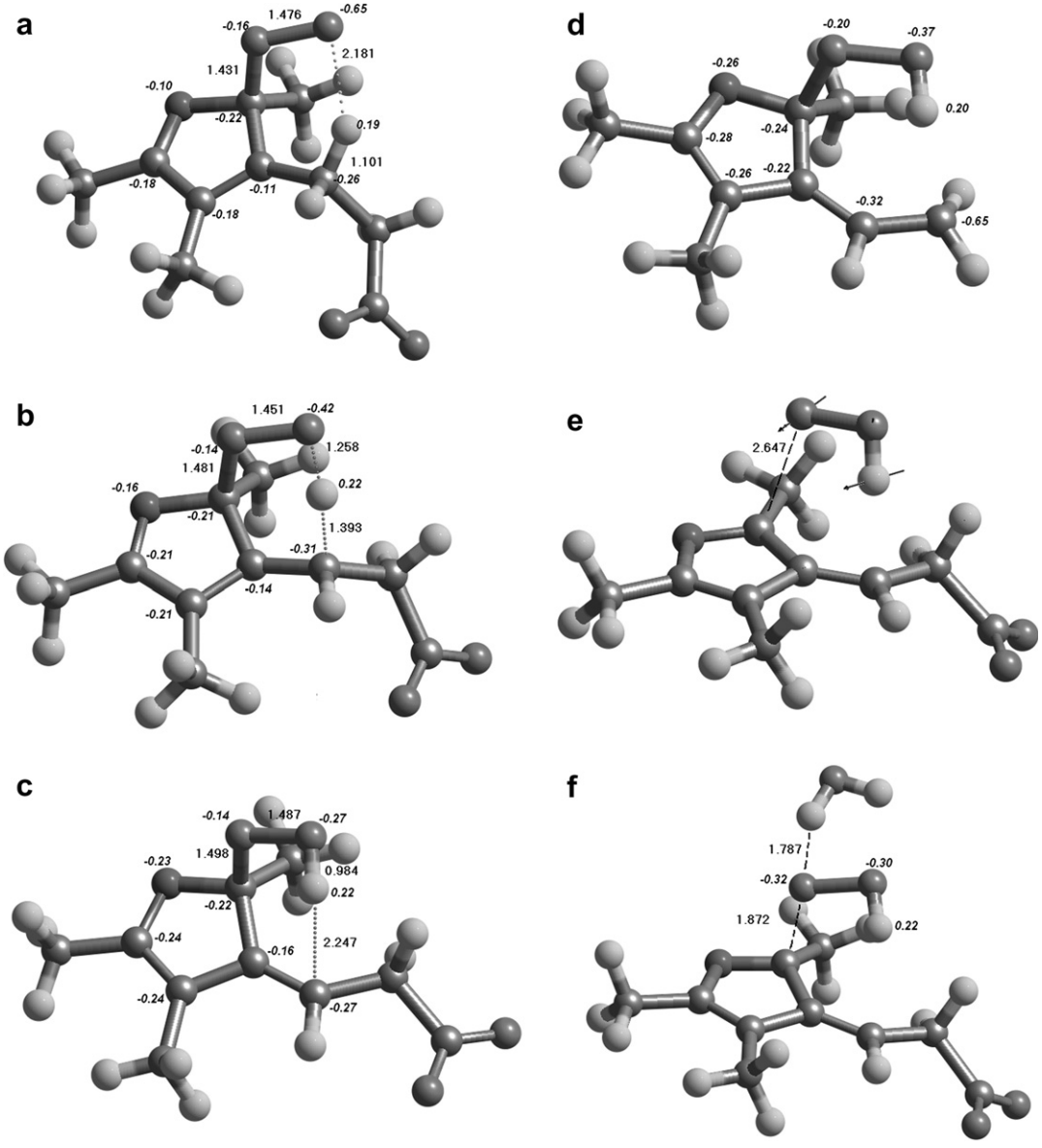

Figure 6. Relevant structures after O_2 addition to N-deprotonated pyrrole. Relevant charges in italics. (a) intermediate 1; (b) transition state 1; (c) intermediate 2; (d) inaccessible intermediate arising from CO_2 elimination from intermediate 2; (e) saddle point found upon distension of the pyrrole-peroxide bond. Imaginary frequency components are shown. Displacement vectors for a methyl group rotation have been omitted for clarity; (f) transition state for peroxide removal from intermediate 2 in the presence of explicit water.

the formation an unusual *spiro*-intermediate (Fig. 7a). Such an intermediate is highly unlikely in the enzyme-catalyzed reaction, since the propionate group is expected to be kept in place through interactions with the substrate-binding pocket present in the enzyme. We therefore estimated the relative energy of the enzyme-bound intermediate by keeping the substrate propionate group in the protonated state (thereby preventing the formation of the gas-phase *spiro* compound) and found it to lie 25.5 kcal mol^{-1} above the reactant state. The transition state for proton removal (Fig. 7b) from the propionate substituent lies at a lower energy (21.6 kcal mol^{-1} above the initial reactants) than the proposed intermediate 1, but markedly higher than that of the deprotonated case discussed above and than the experimental activation energy for the overall reaction. As in the calculations with the deprotonated substrate, CO_2 elimination from intermediate 2 is strongly discouraged: instead, a concerted mechanism is observed, whereby HO_2^- elimination is accompanied by decarboxylation. This concerted transition state (Fig. 7c) lies only 8.3 kcal mol^{-1} above intermediate 2, so that it will not be rate-limiting.

3. Conclusions

Our calculations clearly show that the reaction mechanism of coproporphyrinogen oxidase does not follow Arigoni's one-electron oxidation model with a *protonated* substrate. On the other hand, and although oxygen can be easily reduced to superoxide by N-*deprotonated*

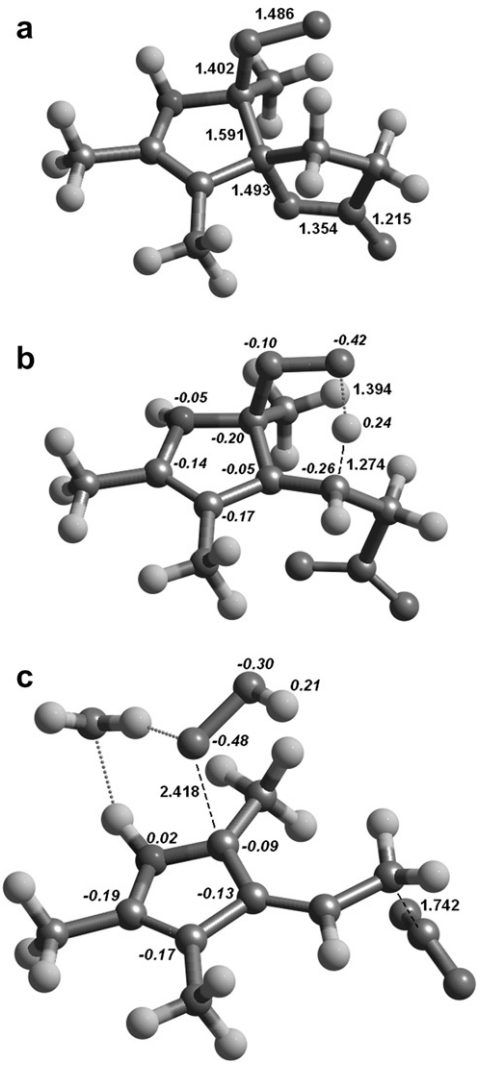

Figure 7. Relevant structures after O_2 addition to N-protonated pyrrole. Relevant charges in italics. (a) gas-phase *spiro* intermediate; (b) transition state 1; (c) transition state for concerted peroxide and CO_2 removal from intermediate 2 in the presence of explicit water.

coproporphyrinogen, superoxide reacts with the coproporphyrinogen cationic radical far too slowly: its activation energy at the low dielectric value of 4 (commonly used in calculations of enzyme-catalyzed reactions) is quite high, at 28.3 kcal mol^{-1}. This value decreases at higher dielectric constants (to 20.8 kcal mol^{-1} at $\varepsilon = 20$ and 19.4 kcal mol^{-1} at $\varepsilon = 78.3$) but it always remains above the barrier computed for the Lash mechanism in the same circumstances (13.5 kcal mol^{-1} at $\varepsilon = 20$ and 13.6 kcal mol^{-1} at $\varepsilon = 78.3$). This difference is not, however, enough to rule out the Arigoni mechanism for the *deprotonated* substrate, as the small size of our model system (due to the limited knowledge about the substrate-binding mode) cannot capture the effect of transition state stabilization by the active site amino acid side chains. The similar energy of the MECP in the Lash mechanism with a deprotonated substrate (11.0 kcal mol^{-1} above reactants, $\varepsilon = 4$) versus that of the Arigoni TS2 (17.8 kcal mol^{-1} above reactants, $\varepsilon = 4$) raises the possibility that the two mechanisms intersect, with the pyrrolyl radical formed in the Arigoni mechanism recombining with the superoxide anion, yielding the 2*H*-pyrrole peroxide anion proposed by Lash, and following the Lash mechanism thenceforth.

The alternative mechanism proposed by Lash affords a potential energy surface (Fig. 8) consistent with the experimental observations, especially if a suitable base is present in the enzyme active site in order to deprotonate the reacting pyrrole ring. However, since the pyrrole nitrogen has a very high p$K_a \approx 15$ and our model did not attempt to capture the energetic cost of the essential pyrrole deprotonation step, we cannot at present discriminate between the N-protonated and N-deprotonated versions of the Lash model. Solving these additional questions must await the availability of a substrate-bound structure of coproporphyrinogen oxidase.

4. Methods

All calculations were performed at the Becke3LYP level of theory.[20–22] Autogenerated delocalized coordinates[23] were used for geometry optimizations, using a medium-sized basis set, 6-31G(d), since it is well known that larger basis sets give very small additional corrections to the geometries, and their use for this end is hence considered unnecessary from a computational point of view.[24–26] More accurate energies of the optimized geometries were calculated with a triple-ζ quality basis set, 6-311+G(2d,p). Zero point (ZPE) and thermal effects ($T = 298.15$ K, $P = 1$ bar) were evaluated using a scaling factor of 0.9804 for the computed frequencies.

The structure of the minimum-energy crossing point (MECP) between non-interacting singlet and triplet states was located at the B3LYP/6-31G(d) level employing the methodology developed by Harvey et al.[27] Since MECP optimization in gas-phase yields very different geometries from continuum MECP optimizations,[28] we performed this search with a PCM continuum model (with $\varepsilon = 4$). State-averaged wavefunctions of the minimum-energy crossing points were converged at the CASSCF(12,8) level (deprotonated state) or the CASSCF(12,9) level (protonated state). The coupling between the two states due to the spin–orbit coupling operator was then computed exactly using the full Breit–Pauli operator.[29] The singlet–triplet transition probability (P) was estimated from the Landau–Zener formula[30]:

$$P = 1 - e^{-2\delta}$$

$$\delta = \pi |H_{ij}|^2 / \hbar v |\Delta g_{ij}|$$

where H_{ij} is the spin–orbit coupling matrix element between the electronic states and Δg_{ij} is the difference of the gradients calculated for the two states at the crossing point. v is the velocity with which the system is passing the crossing region, and in our case cannot be larger than the 418 m s^{-1} calculated from the kinetic theory of gases. Actual values will be much smaller, and therefore our calculated singlet–triplet transition probabilities (P) are over-estimated.

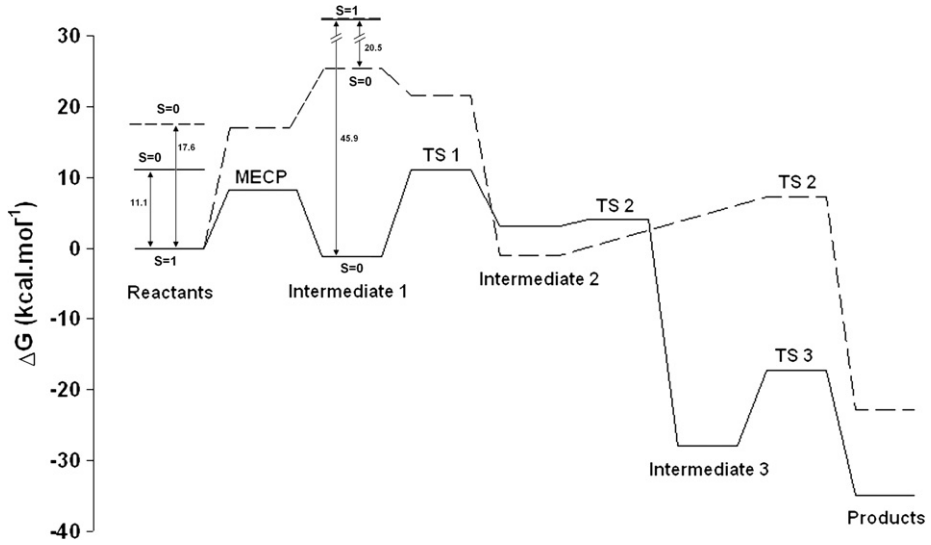

Figure 8. Overall reaction energy profiles of the Lash model at the B3LYP/6-311+G(2d,p)//B3LYP/6-31G(d) level ($\varepsilon = 4$). (—) N-deprotonated substrate; (---) N-protonated substrate. All values except those for the minimum-energy crossing points include zero-point and vibrational contributions. MECP values do not include the contribution due to the avoided crossing (estimated as, at most, 2.4 kcal mol^{-1}).

As computational cost increases very steeply with model size, ring A of the coproporphyrinogen III substrate was modeled as 2,4,5-trimethylpyrrole-3-propionic acid. The substitution of the remaining pyrrole rings by methyl groups is not expected to alter the computational results because these groups play no role in the crucial bond-forming/breaking steps, and their remoteness from the reactive portion of the molecule entails that their inductive effects on electronic distribution in the pyrrole ring should not be much different from those of the (much more computationally amenable) methyl groups. Since the binding mode of the substrate to the enzyme active site is not known, environmental contributions to the stationary points and transition states were computed with the polarizable conductor model,[31–33] as implemented in PcGamess,[34] with a wide range of possible dielectric constants ($\varepsilon = 4$, 20, and 78.3). Unless otherwise noted, all energies mentioned in the text are computed by applying the PCM model ($\varepsilon = 4$) on gas-phase optimized geometries. Dispersion and repulsion effects were evaluated as described by Amovilli and Mennucci.[35] Atomic charge and spin density distributions were calculated with a Mulliken population analysis[36] based on symmetrically orthogonalized orbitals,[37] using the larger basis set. Except for PCM calculations in steps involving paramagnetic species, which were performed with Gamess-US (22nd February 2006 release), all calculations were performed with the PcGamess software package. Computed singlet–triplet gaps were corrected following the procedure described by Ovchinnikov and Labanowski.[38]

Supplementary data

Supplementary data associated with this article can be found, in the online version, at doi:10.1016/j.bmc.2008.01.008. Supplementary Material Available: Geometries of the reactants, transition states, and products of all chemical reactions, as well as correlated orbitals used in CASSCF calculations and spin–orbit evaluation. Energetic profiles computed at different dielectric constants. Relative energies of all intermediates described.

References and notes

1. Sassa, S.; Kappas, A. *J. Intern. Med.* **2000**, *247*, 169.
2. Elder, G. H.; Hift, R. J.; Meissner, P. N. *Lancet* **1997**, *349*, 1613.
3. Tenhunen, R.; Tokola, O.; Linden, I. B. *J. Pharm. Pharmacol.* **1987**, *39*, 780.
4. Elder, G. H.; Evans, J. O.; Jackson, J. R.; Jackson, A. H. *Biochem. J.* **1978**, *169*, 215.
5. Yoshinaga, T.; Sano, S. *J. Biol. Chem.* **1980**, *255*, 4722.
6. Lash, T. D.; Mani, U. N.; Drinan, M. A.; Zhen, C.; Hall, T.; Jones, M. A. *J. Org. Chem.* **1999**, *64*, 464.
7. Akhtar, M. In *The Porphyrin Handbook*; Kadish, K. M., Smith, K. M., Guilard, R., Eds.; Elsevier Science: New York, 2003; Vol. 12, pp 69–86.
8. Medlock, A. E.; Dailey, H. A. *J. Biol. Chem.* **1996**, *271*, 32507.
9. Yoshinaga, T.; Sano, S. *J. Biol. Chem.* **1980**, *255*, 4727.
10. Lee, D.-S.; Flachsová, E.; Bodnárová, M.; Demeler, B.; Martásek, P.; Raman, C. S. *Proc. Natl. Acad. Sci. U.S.A.* **2005**, *102*, 14232.
11. Phillips, J. D.; Whitby, F. G.; Warby, C. A.; Labbe, P.; Yang, C.; Pflugrath, J. W.; Ferrara, J. D.; Robinson, H.; Kushner, J. P.; Hill, C. P. *J. Biol. Chem.* **2004**, *279*, 38960.
12. Lash, T. D. *Bioorg. Med. Chem. Lett.* **2005**, *15*, 4506.
13. Prabhakar, R.; Siegbahn, P. E. M.; Minaev, B. F.; Agren, H. *J. Phys. Chem. B* **2002**, *106*, 3742.
14. Zheng, J.; Wang, D.; Thiel, W.; Shaik, S. *J. Am. Chem. Soc.* **2006**, *128*, 13204.
15. Leopoldini, M.; Russo, N.; Toscano, M.; Dulak, M.; Wesolowski, T. A. *Chem. Eur. J.* **2006**, *12*, 2532.
16. de Visser, S. P.; Ogliaro, F.; Sharma, P. K.; Shaik, S. *J. Am. Chem. Soc.* **2002**, *124*, 11809.
17. Gitter, S. J.; Cooper, C. L.; Friesen, J. A.; Lash, T. D.; Jones, M. A. *Med. Sci. Monit.* **2007**, *13*, BR1.

18. Stephenson, J.R. Stacey, J. A.; Morgenthaler, J. B.; Friesen, J. A.; Lash, T. D.; Jones, M. A. *Protein Sci.* **2007**, *16*, 401.
19. Blomberg, M. R. A.; Siegbahn, P. E. M. *Mol. Phys.* **2003**, *101*, 323.
20. Becke, A. D. *J. Chem. Phys. I* **1993**, *98*, 5648.
21. Lee, C.; Yang, W.; Parr, R. J. *Phys. Rev. B* **1998**, *37*, 785.
22. Hertwig, R. W.; Koch, W. *J. Comput. Chem.* **1995**, *16*, 576.
23. Baker, J.; Kessi, A.; Delley, B. *J. Chem. Phys.* **1996**, *105*, 192.
24. Fernandes, P. A.; Ramos, M. J. *Chemistry* **2004**, *10*, 257.
25. Fernandes, P. A.; Ramos, M. J. *J. Am. Chem. Soc.* **2003**, *125*, 6311.
26. Riley, K. E.; Op't Holt, B. T.; Merz, K. M., Jr. *J. Chem. Theory Comput.* **2007**, *3*, 407.
27. Harvey, J. N.; Aschi, M.; Schwarz, H.; Koch, W. *Theor. Chem. Acc.* **1998**, *99*, 95.
28. Silva, P. J.; Ramos, M. J. *J. Phys. Chem. B* **2007**, *111*, 12883.
29. Fedorov, D. G.; Gordon, M. S. *J. Chem. Phys.* **2000**, *112*, 5611.
30. Nakamura, H. *J. Chem. Phys.* **1987**, *87*, 4031.
31. Tomasi, J.; Persico, M. *Chem. Rev.* **1994**, *94*, 2027.
32. Mennucci, B.; Tomasi, J. *J. Chem. Phys.* **1997**, *106*, 5151.
33. Cossi, M.; Mennucci, B.; Pitarch, J.; Tomasi, J. *J. Comput. Chem.* **1998**, *19*, 833.
34. (a) Schmidt, M. W.; Baldridge, K. K.; Boatz, J. A.; Elbert, S. T.; Gordon, M. S.; Jensen, J. J.; Koseki, S.; Matsunaga, N.; Nguyen, K. A.; Su, S.; Windus, T. L.; Dupuis, M.; Montgomery, J. A. *J. Comput. Chem.* **1993**, *14*, 1347; (b) Granovsky, A. A. PC GAMESS version 7.0, http://classic.chem.msu.su/gran/gamess/index.html.
35. Amovilli, C.; Mennucci, B. *J. Phys. Chem. B* **1997**, *101*, 1051.
36. Mulliken, R. S. *J. Chem. Phys.* **1995**, *23*, 1833.
37. Lowdin, P.-O. *Adv. Chem. Phys.* **1970**, *5*, 185.
38. Ovchinnikov, A. A.; Labanowski, J. K. *Phys. Rev. A* **1996**, *53*, 3946.